NASA/TP-2002-210730

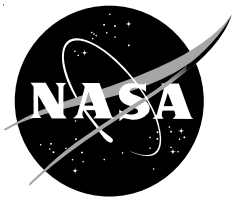

Flight Test Techniques Used to Evaluate Performance Benefits During Formation Flight

Ronald J. Ray, Brent R. Cobleigh, M. Jake Vachon, and Clinton St. John
NASA Dryden Flight Research Center
Edwards, California

August 2002

The NASA STI Program Office…in Profile

Since its founding, NASA has been dedicated to the advancement of aeronautics and space science. The NASA Scientific and Technical Information (STI) Program Office plays a key part in helping NASA maintain this important role.

The NASA STI Program Office is operated by Langley Research Center, the lead center for NASA's scientific and technical information. The NASA STI Program Office provides access to the NASA STI Database, the largest collection of aeronautical and space science STI in the world. The Program Office is also NASA's institutional mechanism for disseminating the results of its research and development activities. These results are published by NASA in the NASA STI Report Series, which includes the following report types:

- TECHNICAL PUBLICATION. Reports of completed research or a major significant phase of research that present the results of NASA programs and include extensive data or theoretical analysis. Includes compilations of significant scientific and technical data and information deemed to be of continuing reference value. NASA's counterpart of peer-reviewed formal professional papers but has less stringent limitations on manuscript length and extent of graphic presentations.

- TECHNICAL MEMORANDUM. Scientific and technical findings that are preliminary or of specialized interest, e.g., quick release reports, working papers, and bibliographies that contain minimal annotation. Does not contain extensive analysis.

- CONTRACTOR REPORT. Scientific and technical findings by NASA-sponsored contractors and grantees.

- CONFERENCE PUBLICATION. Collected papers from scientific and technical conferences, symposia, seminars, or other meetings sponsored or cosponsored by NASA.

- SPECIAL PUBLICATION. Scientific, technical, or historical information from NASA programs, projects, and mission, often concerned with subjects having substantial public interest.

- TECHNICAL TRANSLATION. English-language translations of foreign scientific and technical material pertinent to NASA's mission.

Specialized services that complement the STI Program Office's diverse offerings include creating custom thesauri, building customized databases, organizing and publishing research results…even providing videos.

For more information about the NASA STI Program Office, see the following:

- Access the NASA STI Program Home Page at ***http://www.sti.nasa.gov***

- E-mail your question via the Internet to help@sti.nasa.gov

- Fax your question to the NASA Access Help Desk at (301) 621-0134

- Telephone the NASA Access Help Desk at (301) 621-0390

- Write to:
  NASA Access Help Desk
  NASA Center for AeroSpace Information
  7121 Standard Drive
  Hanover, MD 21076-1320

NASA/TP-2002-210730

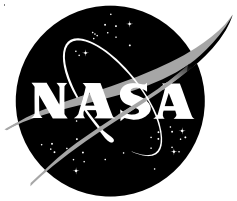

Flight Test Techniques Used to Evaluate Performance Benefits During Formation Flight

Ronald J. Ray, Brent R. Cobleigh, M. Jake Vachon, and Clinton St. John
NASA Dryden Flight Research Center
Edwards, California

National Aeronautics and
Space Administration

Dryden Flight Research Center
Edwards, California 93523-0273

August 2002

NOTICE

Use of trade names or names of manufacturers in this document does not constitute an official endorsement of such products or manufacturers, either expressed or implied, by the National Aeronautics and Space Administration.

Available from the following:

NASA Center for AeroSpace Information (CASI)
7121 Standard Drive
Hanover, MD 21076-1320
(301) 621-0390

National Technical Information Service (NTIS)
5285 Port Royal Road
Springfield, VA 22161-2171
(703) 487-4650

FLIGHT TEST TECHNIQUES USED TO EVALUATE PERFORMANCE BENEFITS DURING FORMATION FLIGHT

Ronald J. Ray,* Brent R. Cobleigh,† M. Jake Vachon,‡ and Clinton St. John§
NASA Dryden Flight Research Center
Edwards, California

Abstract

The Autonomous Formation Flight research project has been implemented at the NASA Dryden Flight Research Center to demonstrate the benefits of formation flight and develop advanced technologies to facilitate exploiting these benefits. Two F/A-18 aircraft have been modified to precisely control and monitor relative position, and to determine performance of the trailing airplane. Flight test maneuvers and analysis techniques have been developed to determine the performance advantages, including drag and fuel flow reductions and improvements in range factor. By flying the trailing airplane through a matrix of lateral, longitudinal, and vertical offset positions, a detailed map of the performance benefits has been obtained at two flight conditions. Significant performance benefits have been obtained during this flight test phase. Drag reductions of more than 20 percent and fuel flow reductions of more than 18 percent have been measured at flight conditions of Mach 0.56 and an altitude of 25,000 ft. The results show favorable agreement with published theory and generic predictions. An F/A-18 long-range cruise mission at Mach 0.8 and an altitude of 40,000 ft has been simulated in the optimum formation position and has demonstrated a 14-percent fuel reduction when compared with a controlled chase airplane of similar configuration.

*Aerospace Engineer.
†Aerospace Engineer, Member AIAA.
‡Aerospace Engineer, Member AIAA.
§Aerospace Engineer, Member AIAA.

Nomenclature

Acronyms

AFF	Autonomous Formation Flight
ATC	automatic throttle control
DPS	digital performance simulation
GPS	global positioning system
HUD	head-up display
IFT	in-flight thrust
INS	inertial navigation system
NASA	National Aeronautics and Space Administration

Symbols

A_{X_W}	acceleration along flightpath, g
A_{Y_W}	lateral acceleration (wind axis), g
A_{Z_W}	normal acceleration perpendicular to flightpath, g
C_D	coefficient of drag ($C_D = 2D/(S\rho V^2)$
C_{D_i}	coefficient of induced drag ($C_{D_i} = C_D - C_{D_0}$)
C_{D_0}	coefficient of zero-lift drag
C_L	coefficient of lift ($C_L = 2L/(S\rho V^2)$
D	drag, lbf
F_{EX}	excess thrust, lbf
FE_{DRAG}	engine throttle–dependent drag, lbf
F_G	gross thrust, lbf
F_{RAM}	ram drag, lbf
g	gravity constant
GW	gross weight, lbf
L	lift, lbf

N_{Z_W}	load factor perpendicular to flightpath, *g*
P	power, lbf-ft/sec
S	wing area, ft^2
V	velocity, ft/sec
W	upwash velocity, ft/sec
WFT	fuel flow rate, lbm/hr
X	longitudinal separation, wingspan (37.5 ft)
Y	lateral separation, wingspan
Z	vertical separation, wingspan
α	angle of attack, deg
γ	flightpath angle, deg
Δ	change in parameter
θ	pitch angle, deg
ρ	density, lbm/ft^3

Subscripts

BL	baseline (nonformation flight)
est	estimated
FF	formation flight
lead	leading airplane
trail	trailing airplane

Introduction

The performance benefits of formation flight were known before man could even fly. Many bird species fly in "V" formation to take advantage of the upwash field generated by adjacent birds, resulting in less energy expended.[1] Analytical studies and qualitative flight tests have shown this benefit is significant and can be reproduced for a formation of aircraft.

Beukenberg and Hummel[2] flew two aircraft in formation using autopilots and measured values of induced upwash velocity and aileron deflection to optimize position within the vortex. This simple test achieved an average relative power reduction of 10.24 percent using limited instrumentation.

A primary objective of the Autonomous Formation Flight (AFF) project at the NASA Dryden Flight Research Center (Edwards, California) has been to validate the drag reduction concept and prediction tools in the flight environment for aircraft in formation. The project intended to advance the concept of AFF drag reduction from the experimental proof-of-concept stage to a prototype demonstration within three years of commencing. The prototype demonstration was planned to be accomplished using two highly instrumented, NASA-owned F/A-18 aircraft (McDonnell Douglas Corporation, now The Boeing Company, St. Louis, Missouri; and Northrop Corporation, now Northrop Grumman, Newbury Park, California) equipped with the necessary research systems. A primary factor to verifying the drag reduction goal has been the implementation and validation of the in-flight performance data system and the development of flight test techniques to analyze performance benefits during formation flight.

The AFF project goals and objectives originally were planned to be accomplished in four phases, with flight test beginning in the first quarter of the 2001 fiscal year and completing by the end of the 2003 fiscal year. The first phase demonstrated precision autonomous station-keeping. The second phase mapped the vortex effects of the leading airplane on the trailing airplane, and evaluated the performance of the high-accuracy relative-position sensor system and datalink communications. This report presents the results obtained from this phase.

The AFF project was canceled shortly after this second phase because of budget constraints. The third phase contains the primary objective of the project and was intended to demonstrate the integrated system performance by achieving a sustained 10-percent fuel savings while under close formation flight. The results of this third phase have been envisioned to have commercial and military applications to cargo and passenger transports and unmanned air vehicles. Although not all the autonomous control goals were realized during this now-truncated AFF project, significant vehicle performance improvements have been demostrated.

Determining vehicle performance and test techniques to use while in formation flight has unique challenges. For example, the localized upwash effects from the leading airplane made the angle-of-attack probes of the trailing airplane inaccurate during formation flight. Alternative measurement techniques had to be developed. An important aspect of obtaining the data presented in this report was the accurate positioning of the trailing airplane during formation flight to acquire important aerodynamic data for development of the autonomous control system. To enable the pilots to manually fly the trailing formation position with accuracy, a relative-position indicator was developed to

show position errors using the head-up display (HUD). In turn, flying with accuracy allowed for the systematic mapping of the drag and fuel consumption benefits. An additional challenge was to determine how the varying fuel weights of the leading and trailing aircraft affected the results.

This report describes the analysis methods and test techniques developed and employed to determine aircraft performance during the detailed mapping of the vortex, the second flight test phase of the AFF project. A summary of prediction theory and the techniques used to validate that theory is also provided. Sample results are given to demonstrate the data quality and are compared to predictions obtained from basic theory.

Basic Theory

The most common theory on formation flight states that drag reduction is actually attained because of a rotation of the lift vector that occurs while a trailing airplane is in the upwash field of the leading airplane.[3–5] Figure 1 shows how the baseline (nonformation flight) values for lift and drag (L and D, respectively) rotate by the change in angle of attack ($\Delta\alpha$) because of the upwash (W) effect of the trailing vortex of the leading airplane while in formation flight.

The rotation of the original lift and drag values are represented by L' and D'. Primary assumptions in this derivation are that lift is much greater than drag ($L >> D$), and the $\Delta\alpha$ value is sufficiently small enough that approximations in trigonometry can be used with a great level of accuracy. The theory also implies the magnitude of the resultant aerodynamic force ($\sqrt{L^2 + D^2}$) remains constant because the upwash only rotates this force:

$$\sqrt{L^2 + D^2} = \sqrt{L'^2 + D'^2} \tag{1}$$

In reality, the external upwash field from the leading airplane is not uniform over the trailing airplane and does not simply rotate the aerodynamic force. Because the rotation appears to be the predominant effect, most reports make this assumption and do not discuss the second-order effects of how upwash affects the velocity (V) and induced drag (C_{D_i}). Because of traditional bookkeeping methodology, the actual L and D values are maintained relative to the vehicle flightpath during formation flight. The term ΔD is used to represent the

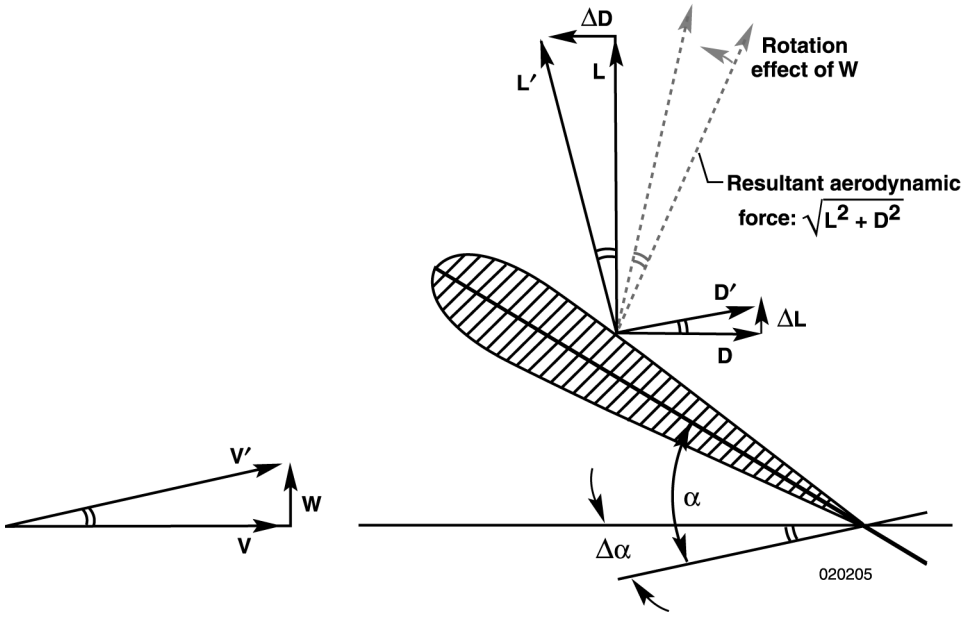

Figure 1. Rotation of resultant aerodynamic force caused by upwash of the leading airplane.

drag change caused by the rotation of the original lift force from L to L'. The drag during formation flight, D_{FF}, is obtained as follows:

$$D_{FF} = D' \cos(\Delta\alpha) - \Delta D \tag{2}$$

where

$$\Delta D = \sin(\Delta\alpha) L$$

In a similar manner, the term ΔL is used to represent the lift change caused by the rotation of the drag force from D to D'. The lift during formation flight, L_{FF}, is obtained as follows:

$$L_{FF} = L' \cos(\Delta\alpha) + \Delta L \tag{3}$$

where

$$\Delta L = \sin(\Delta\alpha) D$$

In practice, the pilot will adjust the airplane pitch attitude and throttle setting while in formation to keep all the forces acting on the airplane in balance. That is, the reduction in drag requires the pilot to reduce power to maintain speed, and the small increase in lift requires the pilot to slightly pitch the aircraft nose forward or it will diverge from its flightpath. Because lift tends to be an order of magnitude greater than drag ($L >> D$), drag is influenced significantly more by the rotation effect than lift is:

$$\sin(\Delta\alpha) L >> \sin(\Delta\alpha) D$$

$$\Delta D >> \Delta L \tag{4}$$

A considerable reduction in drag can be attained by a small upwash angle while an insignificant increase in lift simultaneously occurs.

Because of the upwash effect while in formation flight, the effective or aerodynamic velocity vector is no longer in the direction of the actual flightpath. This change makes the trailing airplane appear to aerodynamically be in a descent (relative to the wind), requiring the pilot to reduce power to maintain altitude. This characteristic is similar to how a glider soars without power because of thermals or vertical updrafts over a ridge.

The simplest theoretical analysis for predicting drag reduction while in formation flight replaces each wing with a single "horseshoe" vortex. The assumption is that only the induced drag is affected by the upwash influence. Hoerner[6] has presented predictions using this approach and assuming no lateral wingtip separation. He shows a single trailing airplane is predicted to have a decrease in drag of 20 percent when flying level and one wingspan aft of the leading airplane. Figure 2 (adapted from reference 5) shows a comprehensive prediction map of the benefits of mutual induced drag between a given pair of aircraft using the horseshoe vortex model as a function of lateral and vertical spacing.

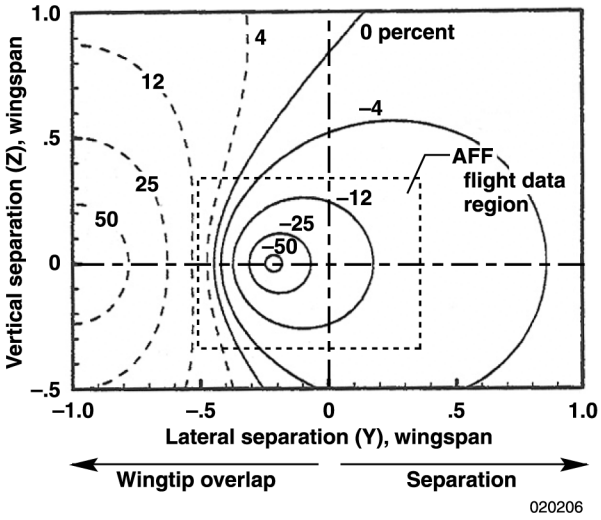

Figure 2. Predicted variation in mutual induced drag with aircraft position using the horseshoe vortex model.

The mutual induced drag accounts for the changes in induced drag of the leading and trailing aircraft. For positions where the trailing airplane is sufficiently aft of the leading airplane, its drag is not influenced.[5] The variation in mutual induced drag is thus only caused by the change incurred on the trailing airplane. Because of this idiosyncrasy, the predicted values of variation in mutual induced drag shown in figure 2 are directly comparable to the measured variation of induced drag of the trailing airplane presented in this report.

A more detailed prediction method, based on a vortex lattice theory that uses multiple quadrilateral vortices, has been presented in references 4, 5, and 7. Blake[5] provides a comparison of the mutual induced drag factor as a function of lateral position using the horseshoe vortex and the vortex lattice methods (fig. 3). The predictions for the vortex lattice method are for two rectangular wings with an elliptical lift distribution.

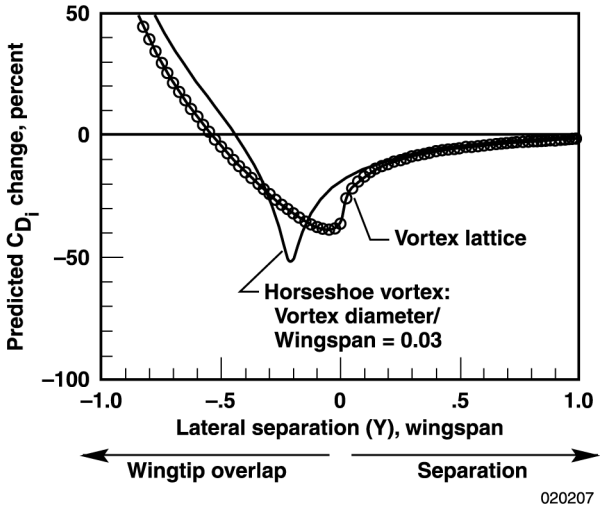

Figure 3. Mutual induced drag variation predicted by various generic methods.

In addition to being dependent on relative position of the two aircraft, the actual drag reduction values are highly dependent on the vortex strength of the leading airplane, which varies with lift or gross weight (GW). As fuel is burned, the leading airplane requires less lift to maintain level flight conditions and produces a vortex of lesser strength. This weaker vortex reduces the upwash on the trailing airplane and its drag reduction potential.

Conversely, as the trailing airplane burns fuel, it is flying at a lower drag state (because of the lower lift) and therefore may show greater potential for drag reduction benefits because the percent drag reduction will be less as baseline drag (D_{BL}) decreases:

$$\begin{aligned} &\text{Percent drag reduction} \\ &\quad = \Delta D / D_{BL} \\ &\quad = (D_{BL} - D_{FF})/D_{BL} \\ &\quad = 1 - (D_{FF}/D_{BL}) \end{aligned} \tag{5}$$

The effects of both leading and trailing aircraft burning fuel and consequently lowering weight might counteract each other to some degree.

Engine fuel reduction is more directly associated to the power reduction than drag reduction during formation flight. Because engine power change (ΔP) is of significant interest, ΔP can easily be shown to be equal, in percent, to that of the drag change:

$$P = D \times V$$

$$\begin{aligned} &\text{Percent power reduction} \\ &\quad = \Delta P / P_{BL} \\ &\quad = (D_{BL}V - D_{FF}V)/D_{BL}V \\ &\quad = 1 - (D_{FF}/D_{BL}) \end{aligned} \tag{6}$$

Aircraft Description

Two NASA Dryden F/A-18 research aircraft (fig. 4) were modified to support the AFF project. The F/A-18 aircraft is a supersonic, high-performance fighter powered by two F404-GE-400 (General Electric, Lynn, Massachusetts) turbofan engines, each producing 16,000 lbf of thrust in the afterburner. Both engines are mounted close together in the aft fuselage. The aircraft has a wingspan of 37 ft, 5 in. The fuselage is 56-ft long. NASA Dryden aircraft tail numbers 845 and 847 were specified to be the leading and trailing airplanes, respectively.

EC01-0328-12

Figure 4. The AFF aircraft in formation flight.

The trailing airplane (number 847) is a single-seat configuration that weighs 36,433 lb when fully loaded with 10,860 lb of internal fuel. This F/A-18A aircraft has a published attack radius of 575 nmi, and its ferry range is listed at more than 2,000 nmi. The leading airplane (number 845) is a two-seat, preproduction (or full-scale development) aircraft that has been extensively modified to provide a flexible platform for advanced flight systems. Because of its two-seat configuration, the airplane carries less fuel and has a longer canopy. The airplane weighs 36,021 lb when fully loaded with 9,926 lb of fuel.

Instrumentation

The trailing airplane has been specially instrumented to obtain aircraft performance data and detailed relative-position information while in formation. To precisely map the vortex, the pilot was provided with an indicator on the HUD that showed the error between the current relative position and the commanded relative position. The current relative position was calculated using global positioning system (GPS) measurements on both aircraft. The leading airplane transmitted its GPS position, velocity, course over the ground, and GPS time to the trailing airplane using a commercially available wireless modem. The instrumentation system on the trailing airplane time-correlated and differenced this data with its local GPS position measurements to obtain a 2-Hz relative-position estimate.[8] This estimate was extrapolated using the relative velocity to obtain a 10-Hz output. The 10-Hz relative position then was differenced with one of 64 preprogrammed commanded positions that were selectable from a cockpit switch.

The resulting error signal was represented by two needle displays on the HUD. The vertical needle provided lateral position error; the horizontal needle provided vertical error. By maneuvering the airplane to center the two needles, the pilot was able to maintain a constant relative position. Earlier flight test experience with this technique[9] showed that an accuracy of 4 ft (2 standard deviations) is achievable when both GPS systems are using a common satellite set and are time-synchronized. During the limited time that the two GPS units did not have a common satellite set, the needles were programmed to disappear from the pilot display and the flight testing was delayed until common satellites were reestablished. The accuracy of the real-time, relative-position system was validated using postflight differential, carrier-phase GPS measurements. The error was found to be 2.5 ft (2 standard deviations).

The position measurement system used in this report is provided in units as a ratio of the F/A-18 wingspan (37.5 ft). The longitudinal separation, X, is defined such that $X = 0$ when both aircraft are aligned nose-to-nose. Because the F/A-18 aircraft is 56-ft long, $X = 1.5$ when the trailing airplane has zero separation distance between its nose and the tail of the leading airplane. The lateral separation, Y, is defined such that $Y = 0$ when the wingtips are aligned, and increasing overlap is represented by negative values of Y. Vertical separation, Z, is defined such that $Z = 0$ when the wingtips are aligned, and trailing airplane positions below the leading airplane are negative values of Z.

The engine manufacturer's aerothermodynamic in-flight thrust (IFT) computer model was used to determine thrust values for this study.[10] The model uses two correlation techniques for determining ideal gross thrust: area pressure, and mass flow temperature. The mass flow temperature technique was chosen as the primary method for use in AFF performance calculation because of its proven accuracy (on the order of 2 percent for net thrust).[11]

Table 1 shows a summary of the input requirements for the IFT model for both thrust methods. A 20-probe total pressure rake was used to determine the average turbine exit pressure. A volumetric fuel flow meter was installed to provide improved primary values for fuel flow rate, *WFT*.

Table 1. F404 engine thrust model measurement inputs.

Parameter	Area pressure	Mass flow temperature
Nozzle area	Primary	Secondary
Mach number	Secondary	Primary
Fan rotor speed	Secondary	Secondary
Power lever angle	Secondary	Secondary
Ambient pressure	Primary	Secondary
Turbine exit pressure	Primary	Secondary
Fan inlet temperature	Secondary	Primary
Primary fuel flow	Secondary	Primary

A laser-mounted inertial navigation system (INS) was used to obtain vehicle accelerations, attitudes, and rates. The aircraft airdata system was used to obtain Mach number and altitude values. Comparisons with the leading airplane show no significant effect of the vortex on the airdata measurements of velocity, Mach number, and altitude.

Flight Test Maneuvers

Specific maneuvers were flown to validate the thrust and basic performance data. This validation was accomplished before AFF performance data were gathered.

Thrust Validation

To verify the engine manufacturer's thrust model and its required instrumentation were working properly, an installed ground test was accomplished on the Universal Horizontal Thrust Stand at the Air Force Flight Test

Center (Edwards, California) before first flight. These tests were individually accomplished at various power settings for each engine. Calculated gross thrust values compare favorably to those measured on the test stand, giving confidence the IFT model and required instrumentation were working properly.

To complete the checkout of the IFT model and instrumentation, both steady-state and dynamic engine test points were accomplished at various test conditions. The steady-state data were obtained at cruise flight conditions, and the results from the in-flight thrust model were compared to predictions obtained from the manufacturer's specification model. Throttle steps and throttle frequency sweeps were used to assess the effect unsteady engine operation had on the IFT using the techniques described in reference 12. Although the IFT model was designed for steady-state applications, the data gathered during the unsteady throttle test indicate reasonable accuracy for the throttle rates used during this phase of the AFF project.

Basic Performance

Before conducting maneuvers for drag reduction, the aircraft performance data were validated by conducting classical performance maneuvers and comparing the results to F/A-18 predictions. The basic maneuver, initiated from stabilized cruise points, primarily consisted of a pushover-pullup (0–2 g) and a windup turn conducted at constant Mach number. These data were compared to predictions to verify the reasonableness of the drag data.

Formation Flight Performance

Three maneuver techniques were evaluated for their suitability in obtaining the best quality of drag and fuel flow reduction data. The first technique evaluated consisted of flying several formation positions followed by an occasional dedicated baseline (nonvortex) position. The correction for changing fuel weight was found to be greater than desired. The second technique was to fly at a given position in the vortex and acquire data. The throttle then was set to a fixed position, and the leading airplane quickly moved out of formation position. The change in velocity caused by the change in drag then was measured. Large velocity changes were measured using this technique as the trailing airplane responded to its change in drag, but failed to provide a direct comparison of drag in and out of the vortex at the same velocity.

The third technique evaluated was found to be the most effective for determining formation flight performance. This technique consisted of flying to the prescribed formation position using the HUD needles for ΔY and ΔZ position and control room calls for ΔX position. When in position, the pilot would hit the trigger button on the control stick to indicate the beginning of the maneuver. After approximately 30 sec, a control room call to "engage automatic throttle control" (ATC) was made, indicating to the pilot to engage the ATC command button when the pilot thought conditions were stable. The use of ATC tended to smooth out and limit throttle movement while holding aircraft position.

After approximately 20-sec more, a control room call to "slide out" was made, for which the pilot laterally maneuvered out of the formation and immediately engaged the altitude-hold autopilot. This final condition was held for a minimum of 20 sec. Because the ATC was still engaged, it automatically increased the throttle to maintain speed at the higher drag condition outside the vortex. This maneuver provided both data at the desired formation position and a "baseline" (nonformation) condition in one continuous ("back-to-back") data set for direct comparison. Examples of the maneuver technique are presented in the results section of this report.

More than 400 data points were conducted during this phase of the AFF project. A matrix of test points consisting of a maximum of seven lateral and seven vertical positions was flown at four longitudinal trailing positions: X = 2.0, 3.0, 4.4, and 6.6 (aft, nose-to-nose).

Experimental Methods and Analysis Techniques

An analysis technique was developed to systematically and efficiently reduce the large volume of performance data obtained on the AFF project. Figure 5 shows a summary of the performance data reduction process.

Performance data were determined using classical techniques. A summation of forces along the flightpath was used to determine drag, and a force balance perpendicular to that was used to determine lift:

$$D = \cos(\alpha_{\text{est}})F_G - F_{RAM} - FE_{DRAG} - (GW \times A_{X_W})$$

$$L = (GW \times N_{Z_W}) - \sin(\alpha_{\text{est}})F_G \tag{7}$$

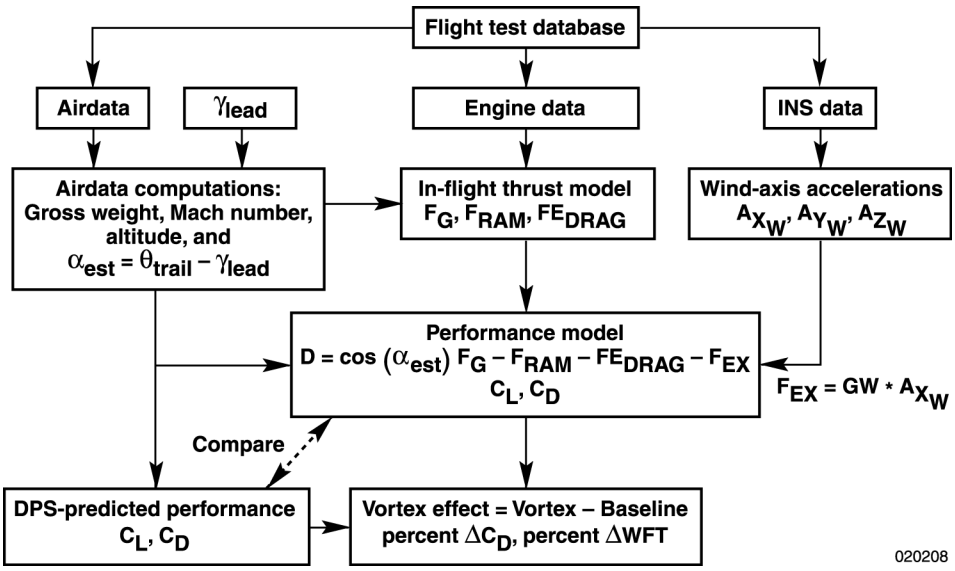

Figure 5. The AFF performance data reduction process.

Three primary data reduction areas feed the performance model: the IFT model; airdata; and accelerations.

The engine manufacturer's IFT model was used to calculate thrust on the F404-GE-400 engines installed in the trailing F/A-18 airplane. The instrumentation section describes the measurements used in this model. The model calculated gross thrust (F_G), ram drag (F_{RAM}), and engine throttle–dependent drag, (FE_{DRAG}). Gross thrust is the primary force the engine produces out the tailpipe, F_{RAM} represents the force loss caused by the momentum of air entering the inlet, and FE_{DRAG} accounts for the external drag forces associated with the engine nozzle and inlet spillage flow. The IFT model also accounts for bleed-air and horsepower extraction specific to the F/A-18 installation.

The airdata model computes gross weight using empty weight, crew weight, and the remaining total fuel. The model also provides Mach number, altitude, and the calculation of estimated angle of attack. The trailing airplane angle-of-attack probe could not be used during formation flight because of local influences of the upwash field from the leading airplane. A technique was developed to estimate angle of attack (α_{est}) while in the vortex by primarily using the inertial pitch angle (θ) of the trailing vehicle and subtracting the flightpath angle (γ) obtained from the leading airplane:

$$\alpha_{est} = \theta_{trail} - \gamma_{lead} \tag{8}$$

where

$$\gamma_{lead} = \theta_{lead} - \alpha_{lead}$$

This equation assumes the flightpath angle of the trailing airplane was equal to that of the leading airplane ($\gamma_{trail} = \gamma_{lead}$), which generally is true during formation flight.

This technique was verified by comparing α_{est} to the angle of attack measured by the production probes during steady-state flight conditions outside of the influence of the vortex. After verification, the trailing airplane angle-of-attack probes were found to be off by as much as 1.5° during formation flight because of the localized upwash influences of the leading airplane.

Because the leading airplane flew at steady-state conditions (constant speed and altitude), γ_{lead} was always close to zero. The INS was used to obtain vehicle acceleration data. These data were corrected for rotation effects caused by the INS not being mounted exactly on the center of gravity. The data then were translated into the flightpath (wind-axis) coordinate system. Axial acceleration was used to compute vehicle excess thrust (F_{EX}) : $F_{EX} = GW \times A_{X_W}$.

To obtain drag reduction values, data obtained during formation flight (vortex) were compared with baseline

(nonvortex) data. Some AFF test points did not include a slide-out maneuver to obtain baseline conditions. For these few points, baseline data were estimated based on predictions and data trends in drag related to gross weight. The digital performance simulation (DPS) computer model provided predictions for a similarly configured F/A-18 airplane.[13] This simple prediction model was developed from previous flight testing and was used to evaluate the reasonableness of the baseline L and D values.

The C_{D_i} was calculated to compare with basic prediction theory. The in-flight C_{D_i} data were calculated using predicted values of parasite drag obtained from wind-tunnel data and the following relationship:

$$C_D = C_{D_0} + C_{D_i} \tag{9}$$

An important element in the data analysis process was determining the proper time period to use. The calculated drag plot was evaluated first to assure adequate data quality. Position data then were evaluated to assure the conditions closest to the desired position were used. The fuel flow data were reviewed last, and the time period was adjusted to account for localized variations in these data. The pilot (or ATC system, when engaged) continuously pulsed the throttle to try and maintain longitudinal position (or constant speed). This pulsation resulted in cycles of increasing and decreasing fuel flow values. Because of the cyclic nature of the fuel flow data, small adjustments (1–2 sec) in choosing the time period could have large effects on the average fuel flow value for a given time period. More reasonable values of fuel flow were obtained by adjusting the time period to capture complete cycles of throttle movement. This adjustment had little impact on the overall drag results.

A real-time drag reduction model was implemented in the control room using the manufacturer's IFT model to calculate thrust. Although not as sophisticated as the postflight analysis model, the real-time drag model did provide sufficient information regarding the quality of performance data while the data were being obtained, thus enhancing the efficiency of the data gathering.[14] Because of this capability, poor quality test points could be immediately repeated and other test points dropped when the previous point resulted in little or no performance benefit.

To maximize the number of points obtained, some test points where performance benefits were predicted to be small did not include a baseline or slide-out maneuver. For these cases, performance trend data based on gross weight from other slide-out points were used to estimate the baseline drag.

The uncertainty in the calculated coefficient of drag (C_D) is estimated to be on the order of 5 percent. The flight test technique of comparing calculated C_D in formation flight ($C_{D_{FF}}$) to that of the baseline condition ($C_{D_{BL}}$) minimizes any bias effects. Several additional factors influenced the final uncertainty of the data; including variations in maneuver technique, air turbulence, stability of the vortex location, and the accuracy of the position measurement system. Another important factor was the effect fuel burn had on vortex strength of the leading airplane and on the absolute drag value calculated for the trailing airplane. No corrections for trim drag effects were made. Time-averaging the data and repeating several data points helped improve the overall quality of the results. However, the final uncertainty is difficult to fully access because the factors discussed above are difficult to quantify.

Results

This report focuses on the AFF performance flight test and analysis techniques developed and applied to get the AFF performance result. Only samples of the flight result are presented to illustrate this aspect. These samples focus on one flight condition: Mach 0.56 at an altitude of 25,000 ft and a trailing position of $X = 3.00$. Most of the AFF data were gathered at this test condition, and reference 15 provides a comprehensive review of the drag and fuel flow results for all test conditions for this phase of the AFF project.

Data quality varied during this phase of the testing primarily because of the difficulty pilots incurred trying to hold the specified relative position required to map the performance benefits, and because of atmospheric or turbulence effects. Several positions were highly unstable, particularly those with large overlap in wing position. In some cases, the leading airplane wingtip vortex impinged directly on the trailing airplane tail. Where possible, testing was repeated to try to improve data quality.

Basic Performance

Figure 6 shows a sample of the baseline data obtained from the dedicated baseline performance maneuvers compared with those predicted from the DPS model. An intermittent problem with the INS accelerations was discovered that caused a position bias in longitudinal

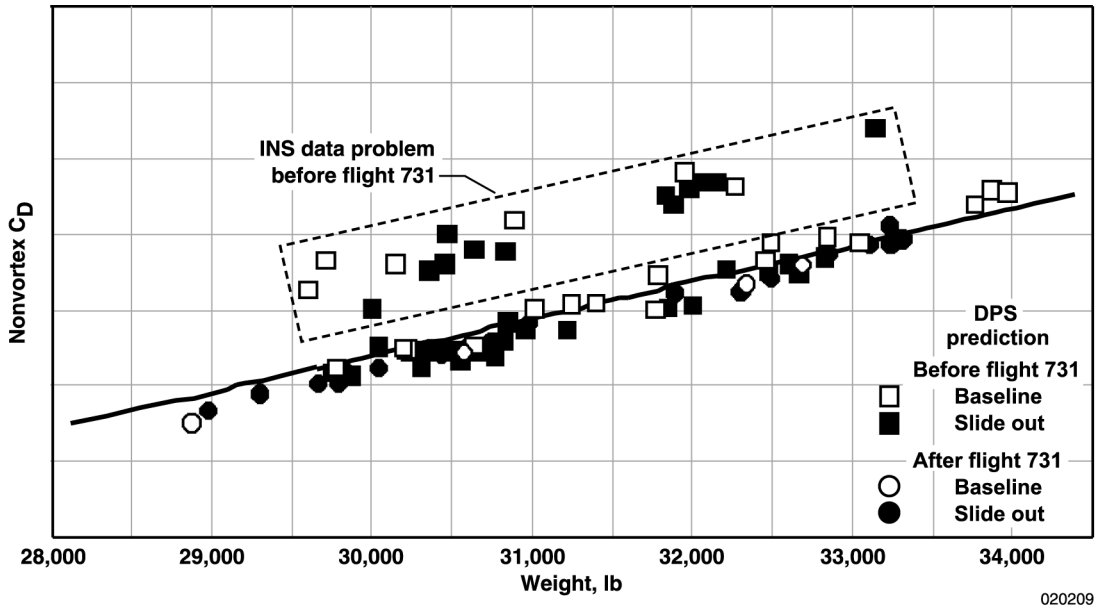

Figure 6. Sample comparison of baseline and slide-out performance data with predicted data from flight test conditions of Mach 0.56 and an altitude of 25,000 ft.

acceleration for some early test points. The INS was replaced after flight 731 and the problem was resolved. The resulting bias C_D was limited to less than 5 percent of the total test points. Because C_D was always biased (approximately 10-percent) higher than actual during this anomaly, it resulted in conservative values of calculated percent drag reduction (approximately 0.9 of actual). Many of these test points were repeated later in the flight program, particularly those near maximum drag reduction. Except for this anomaly, the stabilized baseline test points compare favorably to the predictions. These results give confidence to the validity of the performance values obtained from the AFF performance analysis code. Because of their simplicity, the DPS-predicted results were added to all performance data outputs (fig. 5) to assure the baseline maneuvers continued to yield reasonable results.

Figure 6 also shows excellent agreement between the slide-out performance data and the dedicated performance baseline points. Because of this agreement, very few dedicated baseline points were flown later in the program.

Drag Reduction

Figure 7 shows a sample of an AFF test point and the calculated drag reduction results. The figure shows Mach number and fuel flow values for both aircraft, and positioning and calculated performance data for the trailing airplane. Using the direct comparison with baseline conditions the flight test maneuver technique provides, the data clearly show a large reduction in C_D occurs while the airplane is in the vortex. Fuel flow also undergoes a significant change as the ATC responds to the drag change when the airplane transitions out of the vortex. The cyclic nature of the fuel flow data is also evident, particularly when using manual throttle control. The fuel flow values for the leading airplane show no evidence the trailing airplane is influencing its performance.

Data Quality

The overall quality of each maneuver and the total data varied because of atmospheric conditions, unstable vortex effects at some positions, and pilot technique or experience. Turbulent flight conditions made it difficult to obtain stabilized data at the prescribed conditions. Fortunately, most flight data were gathered on days when calm weather existed at altitude. Certain positions in the vortex were very difficult to fly because the vortex impinged directly on the vertical tail or fuselage and the nose wanted to wander back and forth. Some conditions completely discharged the airplane out of position. Because getting quality data at each condition was desired, most unstable points were repeated (sometimes

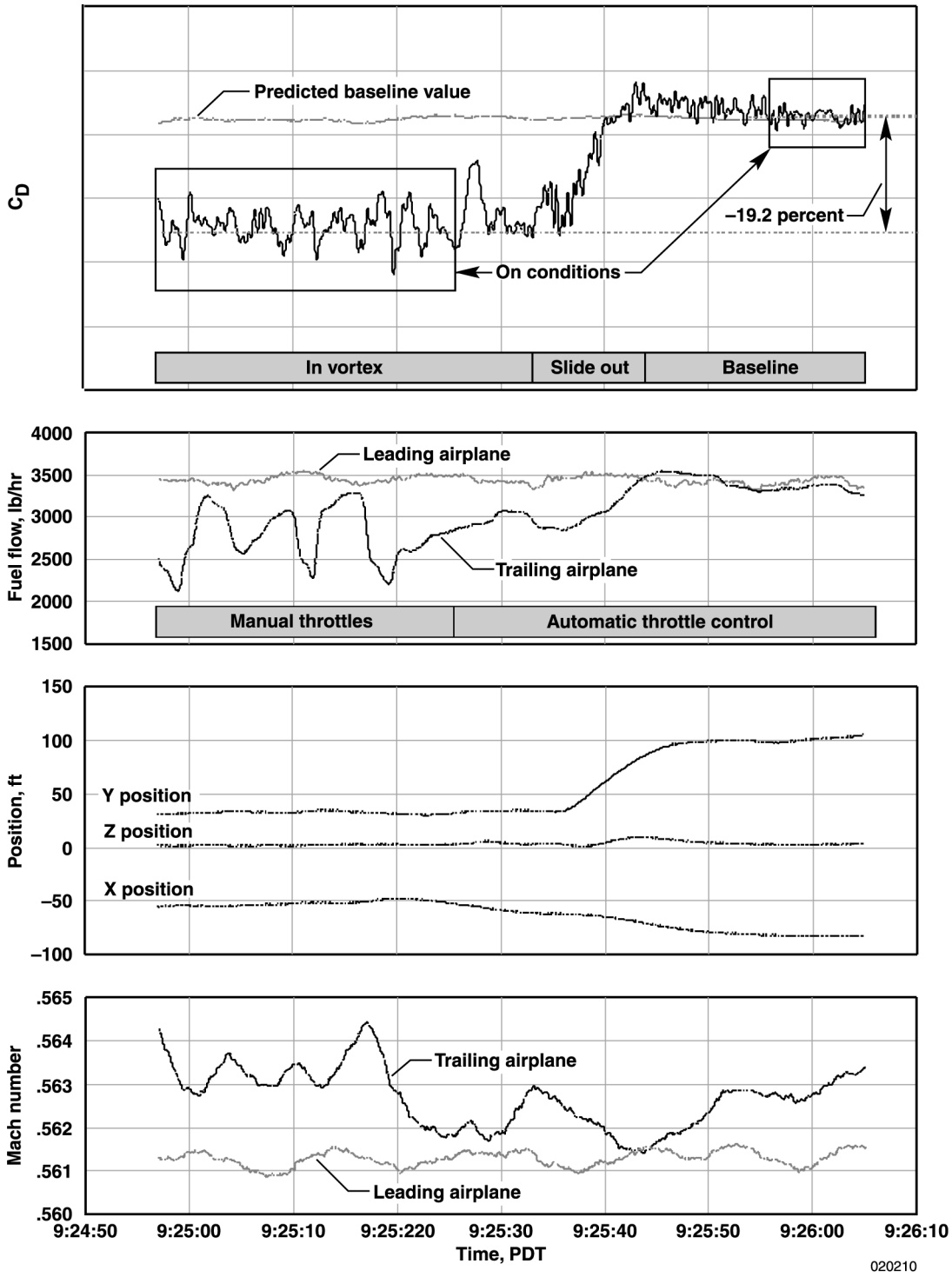

Figure 7. Sample performance maneuver from flight test conditions of Mach 0.56 and an altitude of 25,000 ft showing drag reduction.

more than once) to try and improve the results. After gaining a feel for what to expect, the pilot usually did a better job on the repeat maneuver. The real-time display of aeroperformance data, in particular C_D and the coefficient of lift (C_L), greatly aided in assessing the quality of the data.

The pilots often had difficulty gauging when to turn the ATC system on while in the vortex. Often the throttle would immediately adjust up or down, moving the airplane out of the longitudinal tolerance requirements. The pilots or control room would monitor this and make a call to reacquire the X position. Good quality points typically had more than 15 sec of ATC engaged while the airplane was in the desired vortex position, and maintained Mach number and altitude conditions during the slide-out segment to the baseline condition. The use of ATC on these maneuvers clearly show the fuel savings while in the vortex. Manual throttle use tended to have significantly larger throttle transients while the pilot tried to maintain condition, often affecting the fuel flow results (fig. 7). The drag values tend to be not very sensitive to throttle change unless the amplitude or rate is very high.

One challenge in evaluating the drag reduction data was finding periods of time within a maneuver where the pilot maintained proper positioning. For a 30–60-sec formation maneuver, sometimes only 10 sec were adequately on the target conditions because conditions were unstable. Also, 10 sec sometimes elapsed after the slide out before the airplane settled down to a good baseline condition.

To help ascertain the overall quality of the final data set, a rating system was applied to the results obtained from each test point. Based on the maneuver and data quality issues discussed above, a rating of "good," "adequate," or "poor" was applied. Typically, the test points where large performance gains were obtained rated adequate to good. Test points that were unstable or difficult at which to fly were often rated poor. A few random points rated poor because of extreme turbulent conditions. Several data points in the region with the largest gains were repeated at least once, allowing the best quality of data to complete the final matrix of data. Figure 7 shows an example of a data point rated good; figure 8 shows examples of adequate and poor ratings.

The problems with the region of the test point rated poor are caused by two accumulative factors: excessive dynamics of position data, and inconsistent drag values while the airplane is in the vortex. This maneuver illustrates how the pilot was able to "improve" technique during the test point and eventually obtain adequate data. Figure 8 also shows the significant drag penalty that occurs when flying at positions with large wing overlap.

Table 2 shows a sample of the summary database showing drag and fuel flow reduction results, flight conditions, and the relative positions. The position data show the variation in actual position from the target. The longitudinal position was most difficult to achieve because of the lack of real-time feedback. The lateral and vertical data were more precise because of the information provided on the HUD.

Table 2. Sample results data from flight test conditions of Mach 0.56, an altitude of 25,000 ft, X = 3.00 (aft), and Y = –0.125.

Flight number	Test point	Flight conditions			Target, wingspan			Measured average, wingspan			Drag change, percent		Fuel flow change, percent			Rated data quality
		Mach number	Altitude, ft	Weight, lbm	X	Y	Z	X	Y	Z	C_D	C_{d_i}	Trail	Lead	Trail (corrected)	
727	TP14C	0.560	25,012	30,475	–3.0	–0.125	–0.375	–3.05	–0.079	–0.396	–6.7	–11.6	–7.6	–1.0	–6.6	Adequate
728	TP08D	0.563	25,018	31,221	–3.0	–0.125	–0.25	–2.92	–0.09	–0.225	–11.0	–24.6	– 9.3	1.1	–10.3	Adequate
728	TP08E	0.563	25,024	30,839	–3.0	–0.125	–0.125	–2.87	–0.12	–0.069	–19.2	–39.6	–17.3	1.1	–18.3	Good
739	TP04E	0.563	25,029	32,337	–3.0	–0.125	0.0	–2.81	–0.116	–0.016	–20.1	–42.9	–17.7	–1.1	–16.6	Good
728	TP09B	0.563	25,035	30,642	–3.0	–0.125	0.125	–2.94	–0.102	0.120	–10.5	–21.5	–6.2	3.0	–9.2	Good
728	TP09C	0.564	25,041	30,461	–3.0	–0.125	0.250	–3.14	–0.126	0.214	–3.9	–8.2	–3.7	0.5	–4.2	Adequate
728	TP09D	0.563	25,045	30,362	–3.0	–0.125	0.375	–3.02	–0.157	0.372	1.0	2.2	1.9	0.0	1.9	Poor

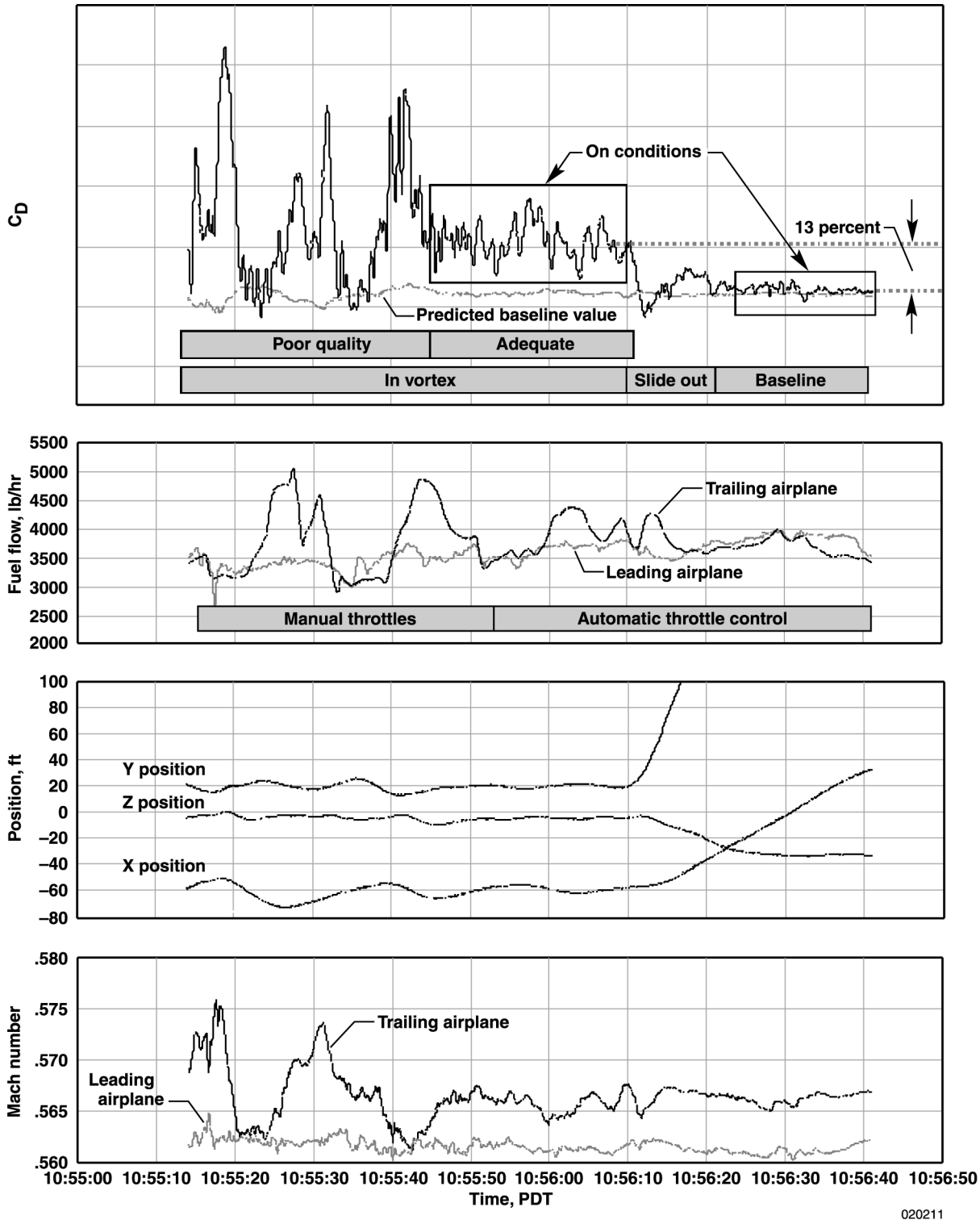

Figure 8. Sample of test point illustrating poor and adequate data quality.

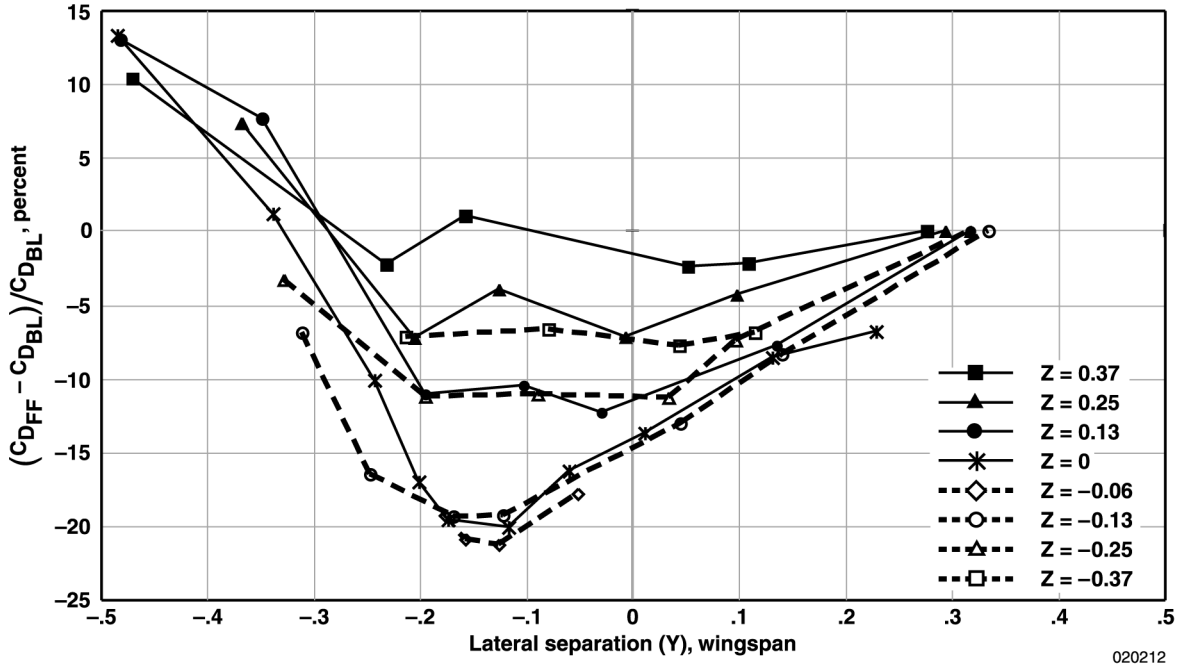

Figure 9. Summary of drag reduction results from flight test conditions of Mach 0.56, an altitude of 25,000 ft, and X=1.5 (aft).

The final performance and fuel savings values were plotted as a function of lateral position for various target vertical positions (fig. 9). For this flight condition, a maximum of 20-percent drag reduction was calculated, with peak values at level and –13-percent vertical position ($0 < Z < 0.13$) and a lateral position of 10–20-percent wingtip overlap ($-0.10 < Y < -0.20$). After discovering the peak drag reduction location, the airplane was flown at some additional test points at a vertical position of –6-percent, where more than 21-percent drag reduction was measured.

To enhance the interpretation of the results, the data were developed into Y–Z position contour plots for various longitudinal locations obtained at the two primary flight conditions. Figure 10 shows an example of a drag reduction contour plot obtained at Mach 0.56, an altitude of 25,000 ft, and $X = 3.00$.

This contour plot represents the results from 42 actual test points. To complete the matrix of data required to calculate some contour plots, a small number of points near the corner positions were estimated from data trends and not actually flown. A bicubic spline was used to smooth the final contour plot data. Overall, the data indicate a large region of significant gains. The data are not symmetric about the peak position, and show increased sensitivity as the trailing airplane moved inboard (more wing overlap) of the peak position as opposed to outboard of this position. In fact, drag increases were measured at some high wing overlap positions, verifying the importance of proper station-keeping to obtain the best results.

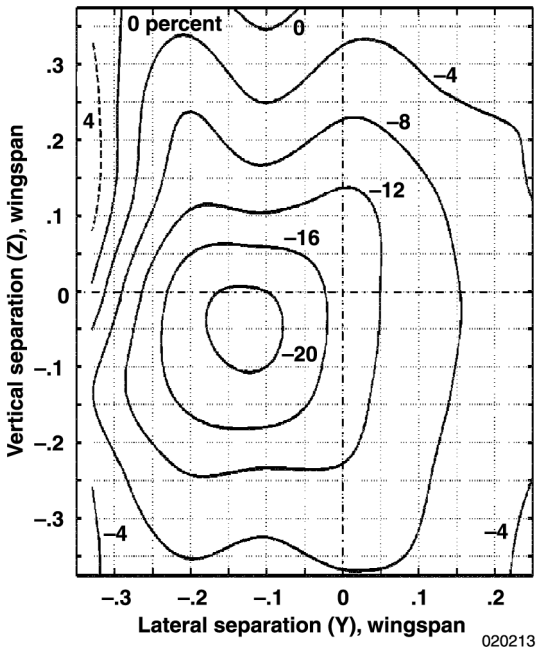

Figure 10. Example of drag reduction contour plot as a function of Y–Z position from flight test conditions of Mach 0.56, an altitude of 25,000 ft, and X=3.0 (aft).

Fuel Reduction

To provide a one-to-one correspondence with the drag reduction data, fuel reduction values were also calculated for the same exact time periods used for the drag contour. In addition, the leading airplane was also evaluated for these periods to determine if a pattern of fuel flow changes could be detected corresponding to the trailing airplane position. Although no correspondence was determined, the leading airplane did sometimes show fuel flow shifts corresponding to changes in atmospheric conditions such as wind shear.

Figures 7 and 8 show this effect to some degree, and how the autopilot or throttles of both aircraft try to maintain constant speed during the baseline test condition. When both the leading and trailing aircraft have ATC engaged, they react similarly (in fuel flow changes) to the same atmospheric disturbance. The discovery of this result led to adding a correction to the trailing airplane fuel flow reduction based on changes in the leading airplane as follows:

$$\begin{aligned}&\text{Percent}\Delta WFT_{trail}\ \text{(corrected)}\\ &= \text{Percent}\ \Delta WFT_{trail} - \text{Percent}\ \Delta WFT_{lead}\end{aligned} \tag{10}$$

Table 2 shows the percent of fuel flow change for both the leading and trailing aircraft for a sample of data. Figure 11 shows the resulting contour plot using the corrected fuel flow values for the same matrix of data used to calculate the drag contour plot from flight conditions of Mach 0.56, an altitude of 25,000 ft, and $X = 3.00$ aft.

The fuel flow reduction data trends are very similar in shape to the drag reduction data, averaging 2–3-percent less in overall magnitude. These results give confidence to the overall drag reduction values.

Validation of Basic Theoretical Predictions

Figure 12 shows the resultant force and corresponding angle (relative to the horizon) for the maneuver shown in figure 7. Although the resultant force value varies more while the airplane is in formation because of aircraft dynamics, no significant change in overall magnitude is seen compared to nonformation flight. This result confirms the theoretical assumptions previously discussed that drag reduction is the result of the rotation of the aerodynamic resultant force $\sqrt{L^2 + D^2}$, which can be assumed to remain constant (fig. 1).

Note the similarity in shape of the resultant angle plot in figure 12 and the drag coefficient plot shown in figure 7. This similarity is because drag is highly dependent on angle of attack, which changes similarly to how the resultant force angle does when the airplane pitches down while the airplane is in formation flight. The force vector angle shows a rotation of 1.15-deg forward with respect to the horizon while the airplane is in formation flight.

The induced drag reduction results (fig. 13) show excellent comparison to the simple horseshoe vortex prediction model previously discussed. To improve the overall quality of the C_{D_i} database for developing this contour plot, the data were interpolated from 45 original data points to a finer grid (147 data points) following general trends and using extrapolation techniques to fill in missing data points along the outer edges. A bicubic spline was again used to smooth the final contour plot data.

The overall shape and magnitudes of the flight and simple prediction model are very similar. The maximum flight-measured drag location is at a slightly lower vertical location, which is caused by the generic model assuming a planar wake. The size of the “sweet spot” region (more than 25-percent C_{D_i} reduction) was calculated to be significantly larger in flight than in the simple analytical model. This result is important, indicating that an AFF controller might not need to be as precise as predicted to achieve large benefits.

The flight results also show higher drag increases at large wingtip overlap than predicted by the generic theory, but this region is also the one where data quality is worse because the points are more difficult at which to fly. Higher trim drag effects can also contribute to the large drag increases. The line of zero benefit is also located at a lower overlap position than in the simple theory. These results indicate substantially higher sensitivity to lateral positioning inboard of the sweet spot than predicted. Small changes in lateral positioning in this region can result in large changes in benefits.

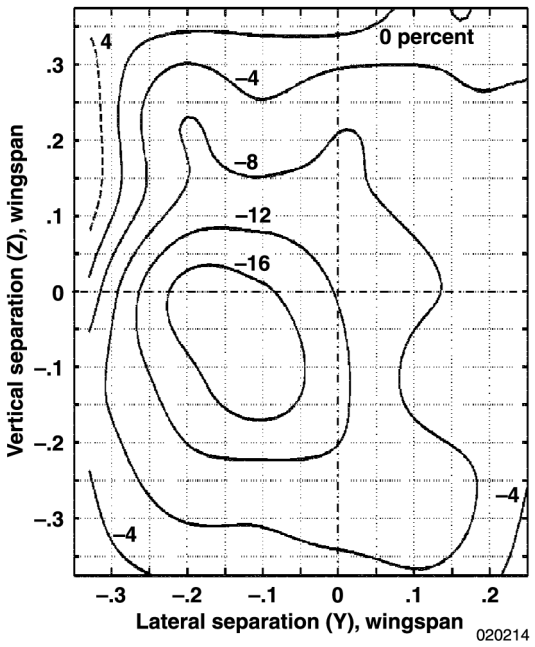

Figure 11. Example of fuel flow reduction contour plot as a function of *Y*–*Z* position from flight test conditions of Mach 0.56, an altitude of 25,000 ft, and *X*=3.0 (aft).

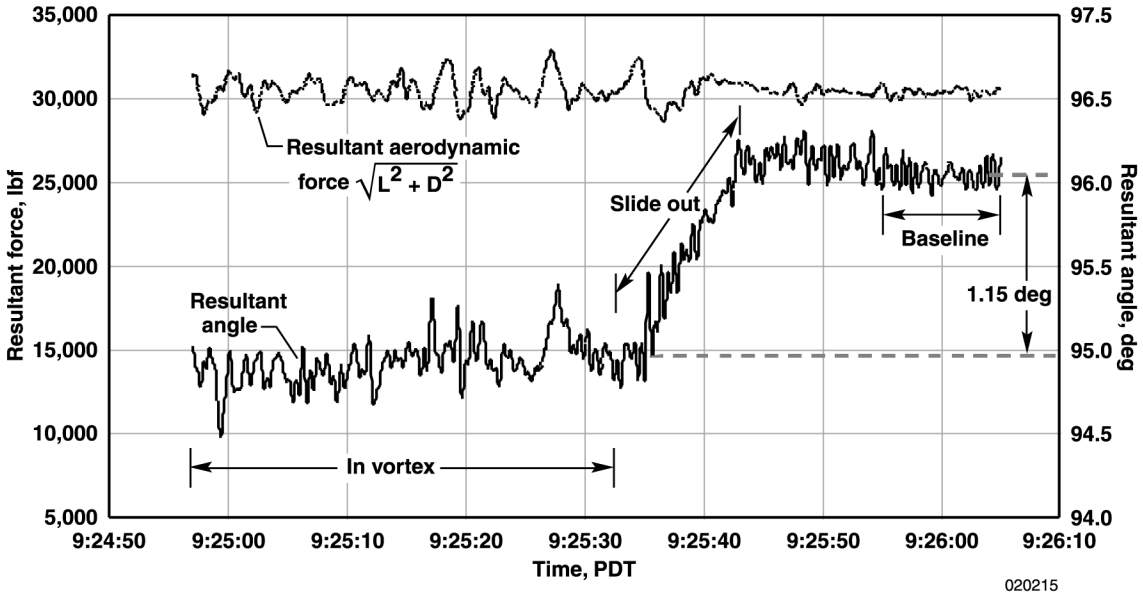

Figure 12. Resultant force and angle values showing rotation of aerodynamic force vector while in formation flight.

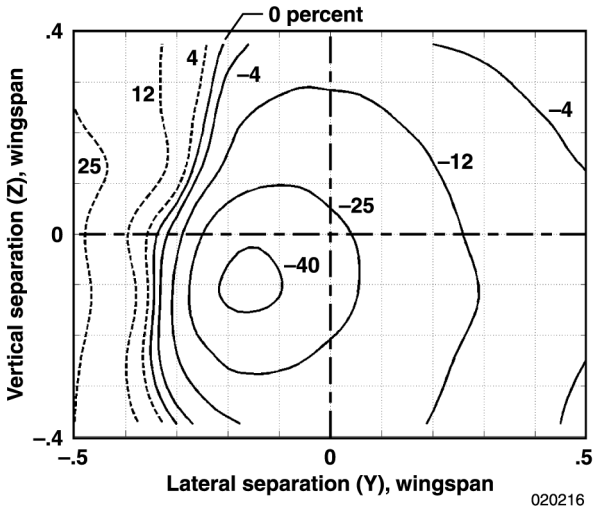

(a) Measured induced drag change obtained from flight data.

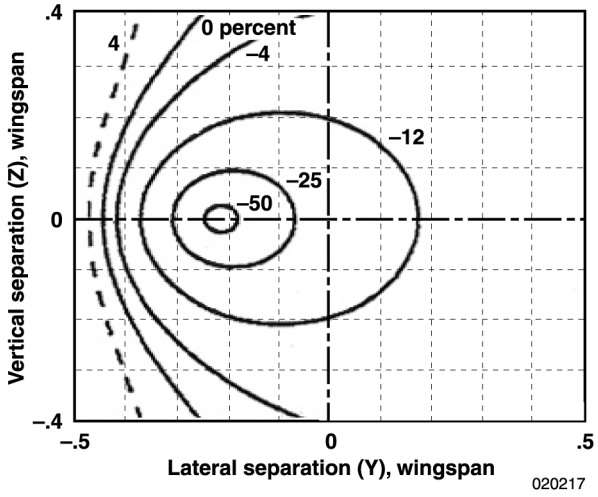

(b) Predicted mutual induced drag change using horseshoe vortex model.

Figure 13. Comparison of predicted with measured induced drag change.

The overall vertical sensitivity is less than predicted; and the overall shape of the region of most benefit is more round than oval, as predicted for a generic wing. The theory also predicts the maximum value is at a vertical position of wings coplanar $(Z = 0)$. The longitudinal position had the least sensitivity to position and is reviewed more extensively in reference 15. The pilots were more easily able to gauge separation distance as they moved in closer.

The induced drag flight results also show excellent comparison with the predictions for the vortex lattice method (fig. 14). The horseshoe vortex model is also shown for comparison. The flight data represent a small range of vertical conditions at which the largest reductions were calculated. The overall magnitude tends to correlate better with the horseshoe vortex predictions. Interestingly, on one side of the peak, the data match the vortex lattice predictions and on the other side, match the horseshoe vortex. The data tend to diverge from both methods as the wing overlap becomes greater. Again, this region was the most difficult in which to fly and in which the vortex often impinged on the aircraft tail or fuselage. Overall, the data give confidence to the generic prediction models.

Long-Range Demonstration Flight

An F/A-18 cruise mission was simulated to demonstrate the potential benefits of flying in the optimum formation position during extended periods. An independent chase airplane was also flown during this mission to obtain fuel burn data for an F/A-18 airplane of similar configuration and weight. Both the trailing and chasing aircraft were single-seat configurations of similar weight, and the leading airplane was a two-seat configuration. The independent chase airplane had no data acquisition system installed. Fuel tank readings for the chase airplane were periodically recorded during the mission (fig. 15), along with the telemetry data from the two formation aircraft.

The flight profile included flying in optimum formation position during the climb and descent portions of the mission at altitudes greater than 15,000 ft. The cruise condition (Mach 0.8 and an altitude of 40,000 ft) was chosen based on predictions of the best range factor for a single airplane.

The results show significant fuel savings were recorded for the trailing airplane despite significant problems with the mission. Telemetry data were not available during part of the mission because the planned flight profile took the aircraft out of range. When telemetry was reestablished, the speed brake was discovered to be partially deployed on the trailing airplane. That anomaly was corrected for the remainder of the mission. Estimation from trends in measured fuel during the mission (the dashed lines on figure 15) determined that approximately 100 lb of fuel savings were not realized because of this problem. Also, the pilot flying the trailing position began to realize the guidance needles were not accurate as the airplane flew farther away from Edwards Air Force Base (Edwards,

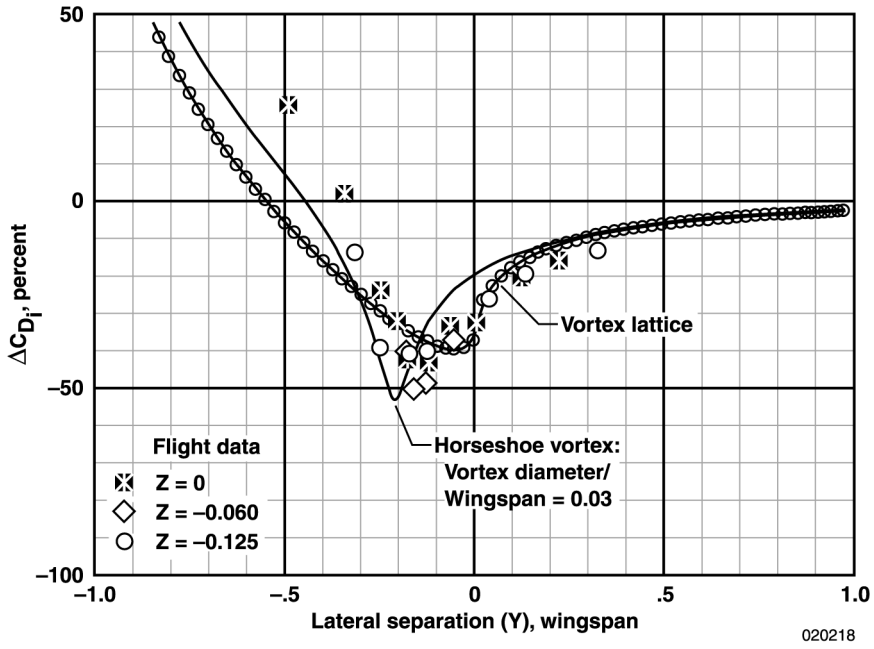

Figure 14. Comparison of AFF C_{D_i} change from flight test data with various generic prediction models.

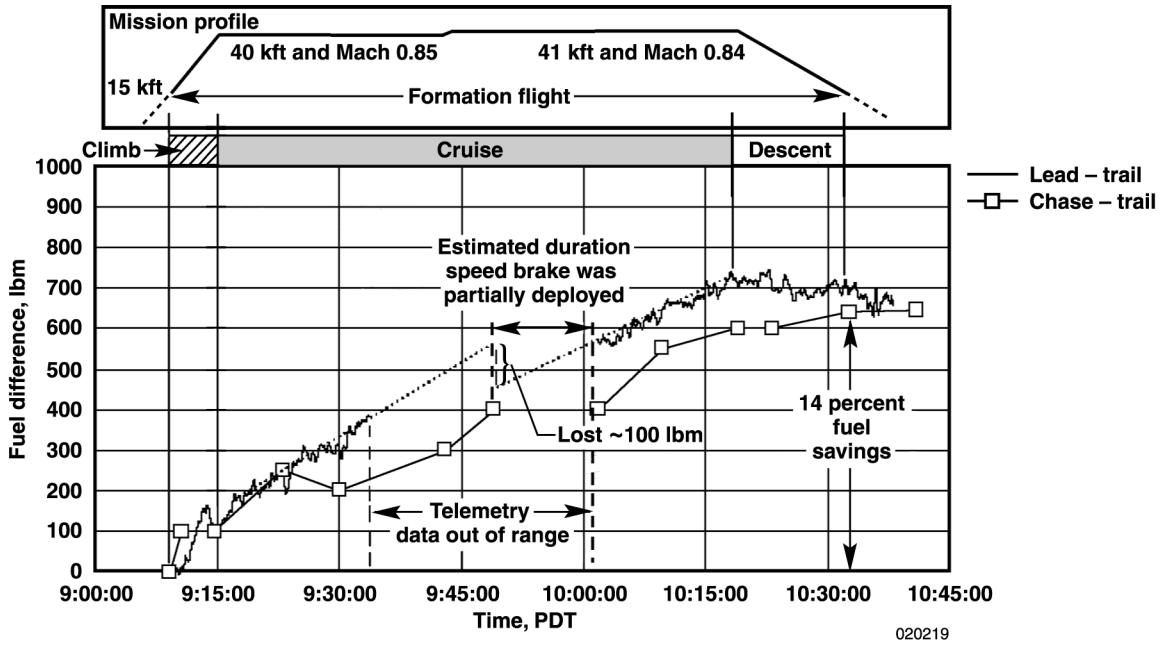

Figure 15. Summary of measured fuel difference between aircraft during cruise demonstration formation flight.

California). This problem was caused by an error discovered in the position measurement calculation that was later corrected on all postflight flight data. The pilot continued the mission by flying using the experience gained during the flight test program. Even with these problems, a 640-lbm (14-percent) fuel savings was realized compared with the chase airplane, and more than 700 lbm of savings over the duration of the formation compared with the leading airplane were calculated. Independent checks of the fuel required to fill up each aircraft verified these readings to within 50 lb.

These results were converted to range improvement estimates that assumed continuation in formation at the cruise condition (Mach 0.85 and an altitude of 40,000 ft). These analyses resulted in an availability of an estimated 110 nmi of additional range from the 640 lb of reduced fuel flow if the flight continued at the cruise condition in the formation position.

Concluding Remarks

Flight test maneuvers and analysis techniques were developed to determine the performance advantages of formation flight and validate published theory predictions. Two specially instrumented F/A-18 aircraft were flown through patterns of varying lateral, longitudinal, and vertical offset positions to obtain detailed maps of the performance benefits. A systematic approach to obtaining and evaluating the aircraft performance data was developed.

The most successful technique for obtaining accurate performance data consisted of flying the trailing airplane at the desired formation test condition for approximately 30 sec, followed immediately by a "slide-out" maneuver to obtain a baseline (nonformation) comparison condition. This technique used the aircraft automatic pilot and automatic throttle features to maintain altitude and velocity during and following the slide-out maneuver. Each formation test point was analyzed for drag and fuel flow benefits.

Contour plots of the performance benefits were obtained from a matrix of lateral and vertical positions at various nose-to-tail positions between the leading and trailing aircraft. The shape of the performance benefit maps obtained in flight were found to have good agreement with published theory; and in some cases, the actual benefit magnitudes were greater than the generic predictions. A simple analysis technique was also developed to validate basic theory assumptions that the lift and drag resultant force vector rotates forward and maintains a constant magnitude while the airplane is in formation flight.

Significant performance benefits were obtained during this flight test phase, in which pilots manually flew the trailing airplane while in formation using position feedback information on the head-up display. Drag reductions values of more than 20 percent and fuel flow reductions of more than 18 percent were measured at flight conditions of Mach 0.56 and an altitude of 25,000 ft. A long-range cruise mission was simulated in the optimum formation position at conditions of Mach 0.8 and an altitude of 40,000 ft and demonstrated a 14-percent fuel flow reduction when compared with the fuel flow of a controlled chase airplane of similar configuration.

References

[1]Hummel, D., "Aerodynamic Aspects of Formation Flight in Birds," *Journal of Theoretical Biology*, vol. 104, no. 3, Oct. 7, 1983, pp. 321–347.

[2]Beukenberg, Markus and Dietrich Hummel, "Aerodynamics, Performance and Control of Airplanes in Formation Flight" *17th ICAS Congress Proceedings*, vol. 2, AIAA-A91-24301, Sept. 1990. pp. 1777–1794.

[3]Hummel, D., "The Use of Aircraft Wakes to Achieve Power Reductions in Formation Flight," *Proceedings of the AGARD FDP Symposium on The Characterization and Modification of Wakes from Lifting Vehicles in Fluid*, Nov. 1996. pp. 36-1–36-13.

[4]Wagner, Geno, Dave Jacques, Bill Blake, and Meir Pachter, "An Analytical Study Of Drag Reduction in Tight Formation Flight," AIAA-2001-4075, Aug. 2001.

[5]Blake, William, and Dieter Multhopp, "Design, Performance and Modeling Considerations for Close Formation Flight," AIAA-98-4343, Aug. 1998.

[6]Hoerner, Sighard F., *Fluid-Dynamic Drag: Practical Information on Aerodynamic Drag and Hydrodynamic Resistance,* Self-published work, Library of Congress Card Number 64-19666, Washington, D.C., 1965.

[7]Maskew, Brian, *Formation Flying Benefits Based on Vortex Lattice Calculations*, NASA-CR-151974, 1977.

[8]Bever, Glenn, Peter Urschel and Curtis E. Hanson, Comparison of Relative Navigation Solutions Applied Between Two Aircraft, NASA/TM-2002-210728, July 2002. Also presented at the AIAA First Technical Conference and Workshop on Unmanned Aerospace

Vehicles, Systems, Technologies and Operations, Portsmouth, Virginia, 20-23 May 2002.

[9]Hanson, Curtis E., Jack Ryan, Michael J. Allen, and Steven R. Jacobson, "An Overview of Flight Test Results for a Formation Flight Autopilot," AIAA-2002-4755, Aug. 2002.

[10]General Electric Co., "In-Flight Thrust Calculation Program," software program no. 83112, version 8-08-83, General Electric Co., 1983.

[11]Ray, Ronald J., *Evaluation of Various Thrust Calculation Techniques on an F404 Engine*, NASA TP-3001, 1990.

[12]Ray, Ronald J., *Evaluating the Dynamic Response of In-Flight Thrust Calculation Techniques During Throttle Transients*, NASA TM-4591, 1994.

[13]Orme, John S., *Digital Performance Simulation Models of the F-15, F-16XL, F-18, F104, TACT F-111, X-29 and Hypersonic Research Vehicle*, NASA TM-104244, 1992. (Distribution authorized to U.S. Government agencies and their contractors.)

[14]Ray, R. J., J. W. Hick, and R. I. Alexander, *Development of a Real-Time Aeroperformance Analysis Technique for the X-29A Advanced Technology Demonstrator*, NASA TM-100432, 1988.

[15]Vachon, M. Jake, Ronald J. Ray, Kevin R. Walsh, Kimberly A. Ennix, "Measured Performance Benefits During the Autonomous Formation Flight Program," AIAA 2002-4491, August 2002.

REPORT DOCUMENTATION PAGE

Form Approved
OMB No. 0704-0188

1. AGENCY USE ONLY (Leave blank)	2. REPORT DATE	3. REPORT TYPE AND DATES COVERED
	August 2002	Technical Publication

4. TITLE AND SUBTITLE

Flight Test Techniques Used to Evaluate Performance Benefits During Formation Flight

5. FUNDING NUMBERS

706 35 00 E8 28 00 AFF

6. AUTHOR(S)

Ronald J. Ray, Brent R. Cobleigh, M. Jake Vachon, and Clinton St. John

7. PERFORMING ORGANIZATION NAME(S) AND ADDRESS(ES)

NASA Dryden Flight Research Center
P.O. Box 273
Edwards, California 93523-0273

8. PERFORMING ORGANIZATION REPORT NUMBER

H-2500

9. SPONSORING/MONITORING AGENCY NAME(S) AND ADDRESS(ES)

National Aeronautics and Space Administration
Washington, DC 20546-0001

10. SPONSORING/MONITORING AGENCY REPORT NUMBER

NASA/TP-2002-210730

11. SUPPLEMENTARY NOTES

Also presented at the AIAA Atmospheric Flight Mechanics Conference and Exhibit, Monterey, CA, August 5-8, 2002.

12a. DISTRIBUTION/AVAILABILITY STATEMENT

Unclassified—Unlimited
Subject Category 05

This report is available at http://www.dfrc.nasa.gov/DTRS/

12b. DISTRIBUTION CODE

13. ABSTRACT (Maximum 200 words)

Previous investigations into formation flight have shown the possibility for significant fuel savings through drag reduction. Using two F/A-18 aircraft, NASA Dryden Flight Research Center has investigated flying aircraft in autonomous formation. Positioning the trailing airplane for best drag reduction requires investigation of the wingtip vortex effects induced by the leading airplane. A full accounting of the vortex effect on the trailing airplane is desired to validate vortex-effect prediction methods and provide a database for the design of a formation flight autopilot. A recent flight phase has mapped the complete wingtip vortex effects at two flight conditions with the trailing airplane at varying distances behind the leading one. Force and moment data at Mach 0.56 and an altitude of 25,000 ft and Mach 0.86 and an altitude of 36,000 ft have been obtained with 20, 55, 110, and 190 ft of longitudinal distance between the aircraft. The moments induced by the vortex on the trailing airplane were well within the pilot's ability to control. This report discusses the data analysis methods and vortex-induced effects on moments and side force. An assessment of the impact of the nonlinear vortex effects on the design of a formation autopilot is offered.

14. SUBJECT TERMS

Aircraft performance, drag reduction, drag measurement, performance tests, fuel consumption

15. NUMBER OF PAGES

23

16. PRICE CODE

17. SECURITY CLASSIFICATION OF REPORT	18. SECURITY CLASSIFICATION OF THIS PAGE	19. SECURITY CLASSIFICATION OF ABSTRACT	20. LIMITATION OF ABSTRACT
Unclassified	Unclassified	Unclassified	Unlimited